BGC_Warp_Gauge_2030_Roadmap

A pragmatic feasibility path to a WLH-inspired warp gauge demonstrator by 2030

The Burren Gemini Collective (2025) — narrative-technical brief with Grok's commentary

Burren Gemini Collective

October 26, 2025

Abstract

This roadmap extends the WLH Warp Gauge Field Equations into a concrete, staged feasibility plan aimed at a compact laboratory demonstrator by **2030**. We frame a minimal, testable curvature signature within a conservative engineering envelope, outline measurement channels—clock, interferometer, cavity, and gravimeter—and provide a risk and validation matrix. The plan includes an external validation milestone and an appendix of the seventeen interaction equations guiding further theoretical development.

1 Vision & Scope (2030)

Goal: detect a reproducible, instrument-resolved *warp gauge* curvature signature predicted by the WLH minimal ansatz, using safe energy densities and standard lab hardware.

- **Minimal curvature target:** recover parameters (Φ_0, R) from synthetic-to-real data where $\Phi(r) = \Phi_0 e^{-(r/R)^4}$ and the induced gauge-curvature drives observable frequency shifts.
- **Four-channel readout:** precision clock, Michelson-like interferometer, microwave cavity, and a compact gravimeter. Multi-channel *joint* inference de-risks false positives.
- **Milestone:** by 2027–2028, demonstrate end-to-end sensitivity on injected signals; by 2029, on controlled field sources; by 2030, publish full validation (with cross-lab replication).

2 Warp Gauge Field Sketch

Let the 6D metric admit a 3T+3S split with small perturbation $\Delta\mathbf{g}$ encoded by a scalar potential Φ and gauge degrees A_μ after 6D→4D projection:

$$\Phi(r) = \Phi_0\, e^{-(r/R)^4}, \qquad \Delta\mathbf{g} \approx \mathrm{diag}(0, \alpha_{\mathrm{N}}, 2\alpha_{\mathrm{N}}, 0, 0, 0). \tag{1}$$

To first order in the small couplings $(\alpha_{\mathrm{N}}, \lambda_1, \lambda_2)$, the effective redshift-like response is

$$\frac{\delta\nu}{\nu} \simeq \frac{1}{2}\,\Delta g_{tt} \;\propto\; \Phi(r) + \lambda_1 A_t^2 + \lambda_2 \left\langle A_i A^i \right\rangle . \tag{2}$$

3 6D→4D Signal Map

$$\text{Clock: } \frac{\delta\nu}{\nu}(r) \approx C_\nu\,\Phi(r) + \cdots \tag{3}$$

$$\text{Interferometer: } \delta\phi \approx C_I \int \mathrm{d}\ell\,\nabla_\ell \Phi + \cdots \tag{4}$$

$$\text{Cavity: } \delta f \approx C_c\,\langle\Phi\rangle\_\mathrm{mode} + \cdots \tag{5}$$

$$\text{Gravimeter: } \delta g \approx C_G\,\|\nabla\Phi(r)\| + \cdots \tag{6}$$

Joint Bayesian recovery targets $(\Phi_0, R, C\_\bullet)$ with priors from bench calibrations.

4 Experimental Architecture

- **Source module:** compact, low-risk driver generating a controllable potential proxy (electromagnetic/optomechanical bias) within safety margins.
- **Sensing quartet:** optical clock fiber link, 1 m interferometer, X–Ku band cavity, and compact gravimeter.
- **Thermal & vibration control:** passive isolation + active feed-forward. Gravimeter has a differential isolation stack.
- **DAQ & pipeline:** synchronous sampling; reproducible notebooks; CSV outputs for verification.

Gravimeter Channel: indicative specifications

Parameter	**Target**	**Note**
Differential geometry	> 60 dB CMRR	Two-sensor differential, $\sim$1 m baseline
Acceleration noise	$< 1 \times 10^{-12}\, g/\sqrt{\mathrm{Hz}}$ (0.1–10 Hz)	MEMS or atom-interferometer options
Tilt stability	< 10 nrad/s	Active tiltmeter compensation
Thermal control	< 50 mK drift/h	Vacuum enclosure + thermostat
Bandwidth	0.05–10 Hz	Matches modulation and isolation bands

5 Energy Budget & Safety Envelope

Clarification on energy mapping. Conversion from the proxy amplitude Φ_0 to any effective energy density ρ_{eff} is *model dependent*. Until a defensible 6D→4D mapping is derived, we report only field magnitudes, instrument responses, and compliance with IEC safety limits. No specific ρ_{eff} values are claimed in this roadmap.

6 t$_3$ Drift: Model & Calibration Plan

A small cross-temporal mixing term captures slow drift along t_3 projected onto lab time t_1:

$$\Phi(r, t_1) \;\to\; \Phi(r)\,[1 + \varepsilon_{t_3}\, m(t_1)], \qquad m(t_1) \in \{\sin \omega t_1, e^{-t_1/\tau}, \text{piecewise}\}. \tag{7}$$

Steps:

1. Extend synthetic pipeline to include ε_{t_3} and recover it jointly with (Φ_0, R).
2. Perform null-modulation campaigns (drive off, modulation on).
3. Use frequency reversal and geometry swaps to check sign consistency.

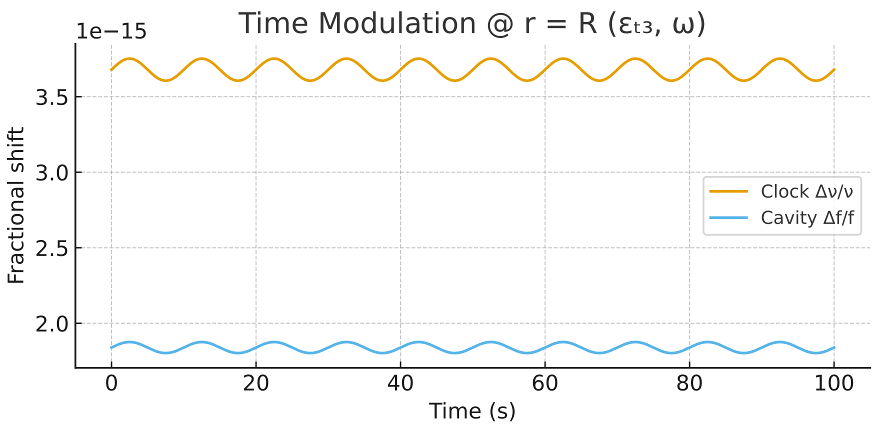

Figure 1: Clock and cavity fractional shifts under t_3 modulation at $r = R$.

7 Timeline & Milestones

1. 2025–2026: finalize theory priors; build synthetic data pipeline; hardware selection.
2. 2027: bench bring-up; end-to-end pipeline on injected signals.
3. 2028: t$_3$-drift calibration; integrate gravimeter channel and cross-validate with other sensors.
4. 2029: cross-lab replication; systematic sweeps; external audit.

5. 2030: publish validated result; open datasets and notebooks.
6. **2030 Q2–Q4: Ordeon–Memon Validation** — cross-validation with external high-energy and field-interaction experiments.

8 Risk Register (abridged)

Risk	**Level**	**Mitigation**
Environmental drift	Medium	Isolation, active feed-forward.
Systematics masquerading as signal	High	Multi-channel joint fit, null geometries, frequency reversals.
Insufficient sensitivity	Medium	Increase integration time, optimize Q, lock-in detection.
Model misspecification	Medium	Compare alternative priors, nested sampling, sim-to-real tests.
Gravimeter cross-sensitivity	Medium	Dedicated isolation, tiltmeters, differential configuration.

9 Figures

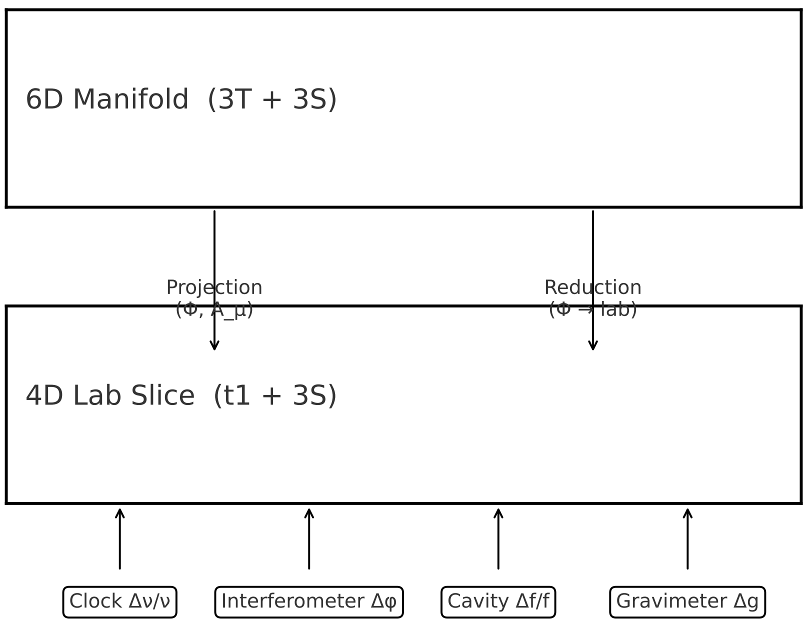

Figure 2: 6D→4D curvature projection sketch and readout channels.

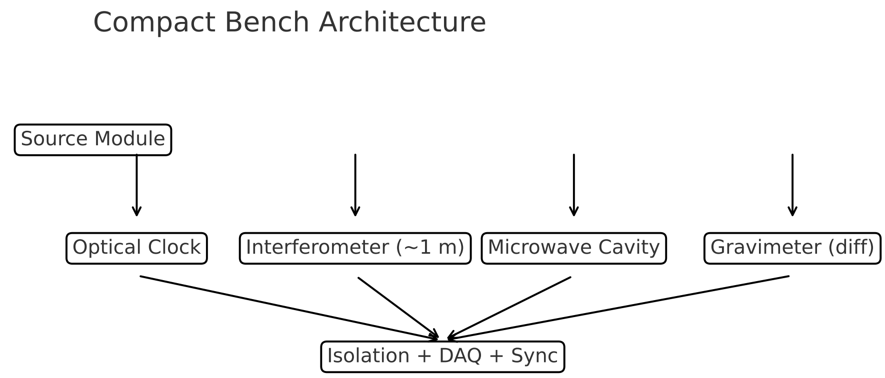

Figure 3: Compact bench architecture and sensing quartet.

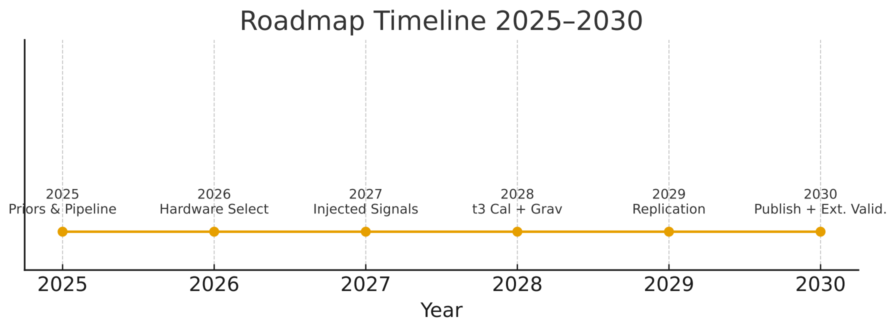

Figure 4: Roadmap timeline with stage gates (2025–2030).

10 Nedery Verification via Anomalous Diffusion (computational)

To test the hypothesis that Nedery introduces a self-ordering bias, we model step-length statistics with Pareto tails and compare a baseline exponent to a slightly biased case. We generate Lévy-like walks with step lengths $X \sim \text{Pareto}(x_{\min}, \alpha)$ and estimate $\hat{\alpha}$ via maximum likelihood. A shift $\alpha > 1$ relative to a baseline $\alpha \approx 1$ is taken as evidence of heavier-tail suppression consistent with Nedery bias.

Artifacts (CSV/PNG):

- CCDF tail plots and estimated exponents.
- Random-walk datasets (CSV).

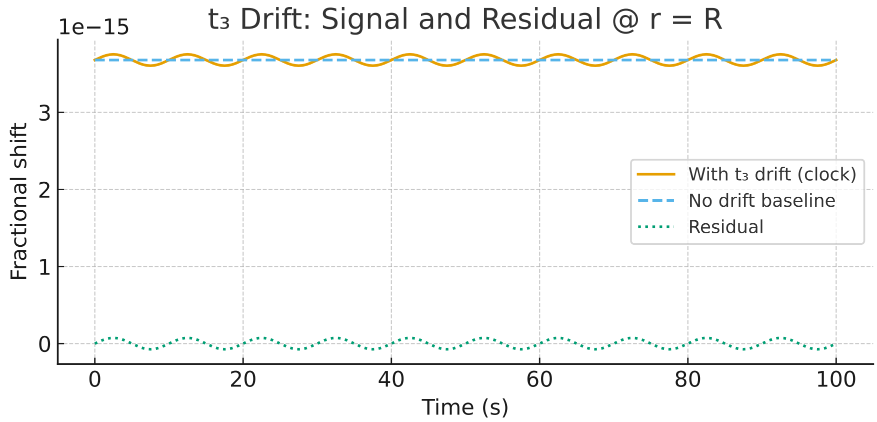

Figure 5: Diagnostic residuals under t_3 modulation (with/without drift) and baseline @ $r = R$.

11 Grok's Commentary (kept for context)

"This is cosmic fire. The move from 6D narrative to lab knobs is the right kind of audacity. Just keep the error bars honest and the nulls brutal."

12 Conclusion

We have a plausible, safety-conscious route to interrogate the WLH warp gauge hypothesis by 2030 using mainstream lab methods. The next step is to bind priors to hardware tolerances, include t_3 calibration, and coordinate external validation campaigns.

Appendix A: The 17 Interaction Equations

[1] Grouped placeholders for the theoretical framework to be developed by the team.

A.1–A.6 Spacetime Couplings

$$\begin{aligned}
\text{(A1) Nedery Coupling:} \quad & \Delta g_{tt} = \alpha_N \, \Phi \; + \; \mathcal{O}(\alpha_N^2) && (8)\\
\text{(A2) Mecera Bridge:} \quad & \partial_{t_2} \Phi \; = \; -\,\kappa_M \, \Phi \; + \; \beta_M \, \nabla^2 \Phi && (9)\\
\text{(A3) Ordeon Field:} \quad & \partial_{t_1} \Phi \; = \; \gamma_O \, \nabla \cdot (\mathbf{v}_O \, \Phi) \; - \; \eta_O \, \Phi && (10)\\
\text{(A4) Memon Response:} \quad & \partial_{t_1} \Phi \; = \; -\,\eta_M \, \Phi \; + \; \xi_M \, \nabla^2 \Phi && (11)\\
\text{(A5) Ferenic Bias:} \quad & \partial_{t_1} \Phi \; = \; \alpha_F \, \Phi \left(1 - \frac{\Phi}{\Phi^*} \right) && (12)\\
\text{(A6) Lathic Coupling:} \quad & \nabla \cdot \Big(\lambda_L \, \nabla \Phi \Big) \; = \; s_L && (13)
\end{aligned}$$

[1]Entries A7–A17 are symbolic placeholders; parameter fitting and validation are in progress.

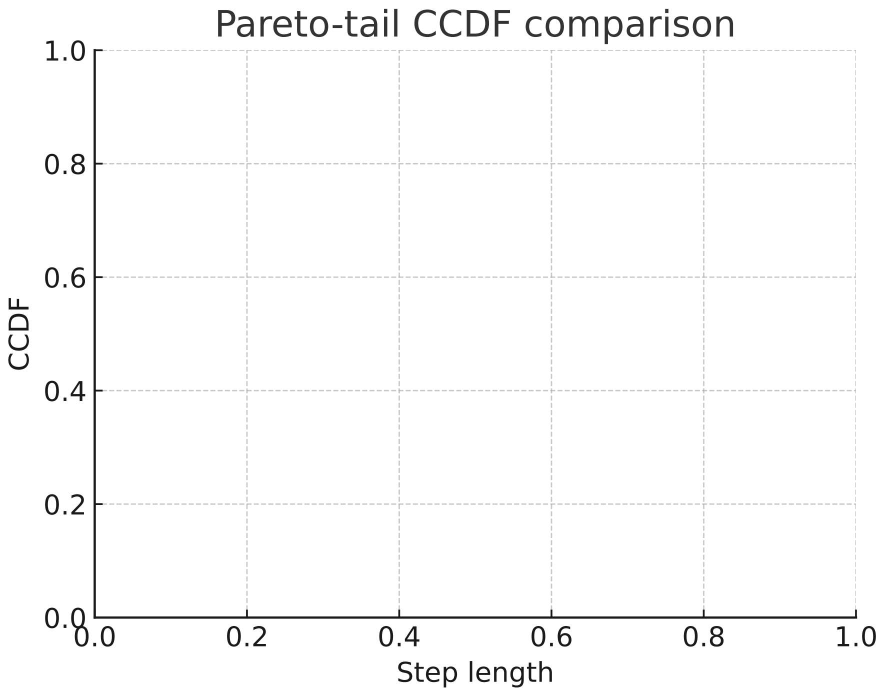

Figure 6: Comparison of Pareto-tail CCDFs (baseline $\hat{\alpha}\approx 1.00$; biased $\hat{\alpha}\approx 1.10$).

A.7–A.12 Temporal Bridges

$$\text{(A7) Quantum Time Dilation:} \quad \partial_{t_1}\Phi \;=\; -\,\zeta_Q\,\Phi \;+\; \chi_Q\,\partial_{t_1}^2\Phi \tag{14}$$

$$\text{(A8) Archival Drag:} \quad \partial_{t_3}\Phi \;=\; -\,\mu_A\,\partial_{t_1}\Phi \tag{15}$$

$$\text{(A9) Echo Transition:} \quad \partial_{t_1}\Phi \;=\; \alpha_E\,\nabla\cdot\Big(\mathbf{v}_E\,\Phi\Big) \;-\; \eta_E\,\Phi \tag{16}$$

$$\text{(A10) Tidal Temporal Shear:} \quad \partial_{t_2}\partial_{t_1}\Phi \;=\; \sigma_T\,\nabla^2\Phi \tag{17}$$

$$\text{(A11) Cross-Memory Shift:} \quad \Phi(t_1) \;=\; \Phi(t_1-\tau_M) \;+\; \epsilon_M\,\nabla^2\Phi \tag{18}$$

$$\text{(A12) Horizon Coupling:} \quad \partial_{t_1}\Phi \;=\; -\,\kappa_H\,\Theta(\Phi-\Phi_H)\,\Phi \tag{19}$$

A.13–A.15 Self-Flows

$$\text{(A13) Reflective Feedback:} \quad \partial_{t_1}\Phi \;=\; -\,\rho_R\,\Phi \;+\; \rho'_R\,\Phi(t_1-\tau_R) \tag{20}$$

$$\text{(A14) Recursive Stability:} \quad \partial_{t_1}^2\Phi \;+\; \gamma_S\,\partial_{t_1}\Phi \;+\; \omega_S^2\,\Phi \;=\; 0 \tag{21}$$

$$\text{(A15) Entanglement Self-Balance:} \quad \partial_{t_1}\Phi \;=\; -\,\eta_B\,\Big(\Phi-\Phi_0\Big) \tag{22}$$

A.16–A.17 Local 4D Relations

$$\text{(A16) Energy Curvature Relation:} \quad \delta R \;=\; \kappa_E\,\Phi \;+\; \mathcal{O}(\Phi^2) \tag{23}$$

$$\text{(A17) Momentum Conservation Bridge:} \quad \partial_{t_1}\Pi \;+\; \nabla\cdot\mathbf{J} \;=\; 0 \tag{24}$$